



Evaluation of SEBS and SEBAL algorithms for estimating wheat evapotranspiration (case study: central areas of Khuzestan province)

Elahe Zoratipour¹ · Amir Soltani Mohammadi¹ · Amin Zoratipour²

Received: 16 February 2023 / Accepted: 8 May 2023 / Published online: 22 May 2023
© The Author(s) 2023

Abstract

This study aimed to accurately estimate daily wheat evapotranspiration using two remote sensing algorithms, Surface Energy Balance System (SEBS) and Surface Energy Balance Algorithm for Land (SEBAL), in central Khuzestan province during 2019–2020. The results of two algorithms were compared with lysimeter (as a direct method), FAO-Penman–Monteith (FAO-PM), two temperature-based methods (Hargreaves-Samani and Blaney-Cridde), two radiation-based methods (Priestley–Taylor and Doorenbos–Pruitt), and two mass transfer-based methods (Mahringer and World Meteorology Organization) (as indirect methods). Coefficient of Determination (R^2), Root-Mean-Square Error (RMSE), Percentage of Bias (PBIAS), Mean Bias Error, Mean Absolute Percentage Error, and Nash–Sutcliffe indicators used for comparing the results. According to the results, both SEBAL and SEBS algorithms showed the highest compatibility with lysimeter data ($R^2=0.92$ and 0.96 , RMSE = 2.15 and 1.53 mm/day, respectively). Comparing both algorithms with the FAO-PM method, resulted in RMSE and R^2 of 2.42 mm/day and 0.87 for SEBS and 3.14 mm/day and 0.79 for SEBAL. The Hargreaves-Samani method ($R^2=0.72$, RMSE = 16.4 mm/day) and ($R^2=0.8$, RMSE = 10.4 mm/day) among temperature-based methods, Doorenbos–Pruitt ($R^2=0.71$, RMSE = 3.33 mm/day) and ($R^2=0.79$, RMSE = 2.63 mm/day) among radiation-based methods, and the Mahringer method ($R^2=0.6$, RMSE = 6.8 mm/day) and ($R^2=0.68$, RMSE = 5.51 mm/day) among mass transfer-based methods yielded better estimations than SEBAL and SEBS algorithms, respectively. Owing to the high accuracy of SEBAL and SEBS algorithms, in estimating the amount of evapotranspiration in the study area and close to the actual values in the field, using energy balance algorithms is recommended in Khuzestan province.

Keywords Evapotranspiration · Lysimeter · FAO-Penman–Monteith · Remote sensing

Introduction

Crop evapotranspiration (ET) plays a key role in determining crop water requirements and ultimately correctly designing irrigation systems (Djaman et al. 2015). ET is a major component of water balance, and its accurate estimation is

of great importance in water use planning and optimization (Asadi et al. 2022). It is also necessary for irrigation and water resources management, increasing yield, and better crop management (Shamloo et al. 2021). ET is correctly estimated using different methods, the accuracy of which depends on the climatic conditions of the study areas (Racz et al. 2013). The actual ET can be measured directly using the water balance method, which is often a costly and complicated technique, but it is considered an effective tool for the validation and calibration of ET estimation models. Although indirect methods, such as mathematical models for ET estimation, can be employed easily, they are used when measurement methods are difficult (Obada et al. 2017). Based on the literature, conventional ET estimation methods are classified into three main groups, namely temperature-based, radiation-based, and mass transfer-based methods (Xu and Singh. 2002). In the FAO-Penman–Monteith (FAO-PM) method, the weather parameters are considered related

✉ Amir Soltani Mohammadi
A.soltani@scu.ac.ir
Elahe Zoratipour
elahezoratipour@gmail.com
Amin Zoratipour
Zoratipour@asnruk.ac.ir

¹ Faculty of Water and Environmental Engineering, Shahid Chamran University of Ahvaz, Ahvaz, Iran

² Department of Nature Engineering, Agricultural Sciences and Natural Resources University of Khuzestan, Mollasani, Iran

to these three categories (Obada et al. 2017). Climatic data are limited in most areas, and it is not the ability to use the FAO-PM method; thus, other methods are recommended for ET calculation (Djaman et al. 2015). Remote sensing makes it possible to obtain the amount of daily ET in different areas, with wide scales at the least possible time and with high economic benefit (Saboori et al. 2021).

Most RS-based Surface Energy Balance algorithms have been developed for crop ET determination in specific conditions in terms of land use and crop management, considering the accordance of empirical functions and parameters with these algorithms (Wolff et al. 2022). They are easily used in accurate agricultural management systems for better decision-making and higher yields (Shamloo et al. 2021). To determine actual crop ET, many temperature-based, radiation-based, and mass transfer-based empirical methods were compared with FAO-PM and lysimeter methods in different climatic and spatial conditions. This indicates the importance of crop ET estimation, including cereals, to determine crop water requirements and the optimal use of water resources. In this context, Djaman et al. assessed 16 ET methods under coastal conditions in the Senegal River Delta, and the results indicated the good performance of the Mahringer and Terabert methods (Djaman et al. 2015). Lang et al. compared eight ET estimation methods with the FAO-PM method in southwest China. The results revealed that the performance of these methods was dependent on the regional climate type in each area. However, the best performance was reported for Makkink and Hargreaves-Samani methods from radiation and temperature-based methods, respectively (Lang et al. 2017). Zoratipour et al. studied the spatial and temporal evaluation of different methods for the prediction of ET in Khuzestan province. According to the results, the best ET estimations in this province were recorded for the Hargreaves-Samani among the temperature-based method, Doorenbos–Pruitt among the radiation-based method, and Mahringer and the World Meteorological Organization (WMO) among the mass transfer-based methods (Zoratipour et al. 2019). Empirical methods have limitations due to the need for measuring all effective parameters at more time and higher cost for the necessary equipment preparation and agricultural operations; also it is not easy to measure soil water balance data at depths. Given the limitations of various empirical methods, the possibility of errors in field measurements, and their non-allocation to large extents, the results can be feasibly extended with a combination of land and RS data as a Surface Energy Balance model. Accordingly, Lian et al. estimated wheat ET in the Heihe River basin based on Landsat8 satellite imagery and Mapping ET at High Resolution with Internalized Calibration (METRIC) algorithm, which was reported to be able to present accurate estimations in various heterogeneous land uses (Lian and Huang 2015). Rawat et al. determined wheat crop ET using

the SEBAL model in the India. The results demonstrated that the SEBAL-based ET conformed with lysimeter method with R^2 value of 0.91 (Rawat et al. 2017). Wang et al. in the Heihe River Basin, Northwestern China, estimated daily ET using the SEBS algorithm, and assessed its performance with Eddy Covariance and Priestley-Taylor methods. The results revealed that the SEBS model has a relatively accurate performance, particularly for vegetated areas (Wang et al. 2017). Elnmer et al. studied daily ET of crops, using the SEBAL algorithm compared to the FAO-PM method, in the Nile Delta, resulting in an RMSE of 0.46 mm (Elnmer et al. 2019). Ghaderi et al. estimated wheat ET, using the SEBAL algorithm and Landsat 8 satellite images in Ilam province. Compared to the FAO-PM method, the SEBAL algorithm demonstrated adequate precision for ET estimation. They obtained the Root-Mean-Square Error (RMSE), Mean Absolute Percentage Error (MAPE), Mean Bias Error (MBE), and Coefficient of Determination (R^2) at 0.46, 2.9%, 0.22 mm/day, and 0.97, respectively (Ghaderi et al. 2020). Tan et al. estimated ET based on the SEBAL algorithm by using RS and Landsat 8 images upstream of the Heihe River Basin in China. The algorithm performance was evaluated using four empirical methods Irmak, Turc, FAO-PM and Jensen-Haise. The results indicated that the SEBAL algorithm could present accurate ET estimations in the studied area (Tan et al. 2021). Khand et al. assessed wheat ET modeling based on SEBAL, METRIC, and SEBS algorithms and obtained a smaller RMSE (0.14 mm/day) for the METRIC model than those of SEBAL and SEBS algorithms (Khand et al. 2021). Shamloo et al. evaluated the SEBS algorithm to estimate maize ET and crop coefficient using Landsat 8 images in the Adana Mediterranean Area, Turkey. According to the results, the SEBAL estimated ET values mostly corresponded to the FAO-PM method with $R^2 = 0.91$ and RMSE = 1.14 mm/day. It was also highly correlated with Turc, Hargreaves, and Makkink methods (Shamloo et al. 2021). Asadi et al. compared actual wheat crop ET based on SEBAL algorithm using 12 Landsat 7 and Landsat 8 images during the crop development period in the Parsabad Moghan Plain, Northwestern Iran. The results demonstrated that the SEBAL algorithm (RSME = 0.633 mm/day and $R^2 = 0.93$) had the minimum error rate and maximum similarity compared to lysimeter data (Asadi and Valizadeh Kamran. 2022). Yang et al. investigated actual ET in different land uses based on the SEBAL algorithm and landsat 8 images in Ecotone, Northwestern China. The SEBAL algorithm had an appropriate estimation (RMSE = 0.9 mm/day and $R^2 = 0.81$), which was suitable for research on water resources, but it overestimated ET (Yang et al. 2022). In another study, Wei et al. evaluated daily ET estimation of rice fields, using the SEBAL algorithm in a subtropical region in Southern China. The results showed a high precision of the SEBAL algorithm, on a daily scale, with R^2 , NSE, and RMSE values

of 0.85, 0.81, and 0.84 mm/day, which confirmed SEBAL application to logically allocate water resources in subtropical regions (Wei et al. 2022). Tariqul Islam et al. determined actual wheat evapotranspiration by the lysimeter method and SEBAL algorithm using Landsat 8 and Sentinel 2 satellite images. The results concluded the ET of wheat estimated by SEBAL had maximum similarity compared to lysimeter data. Also the average seasonal wheat ET was calculated to be 253 mm (Tariqul Islam et al. 2023). Liu et al. used the SEBS algorithm and Landsat 8 satellite images to estimate regional evapotranspiration in Beijing. The results showed that ET decreased with increasing land surface temperature (LST) and daily evapotranspiration ranged from 3.47 to 5.47 mm (Liu et al. 2023). Khoshnood et al. evaluated SEBS algorithm to investigate the rate of evapotranspiration change in different land cover use classes in the entire Urmia lake basin from 2016 to 2020. They stated that there is a high correlation between the results of the SEBS algorithm and the values measured (Khoshnood et al. 2023).

ET evaluation in every region and choosing the best methods tailored to each weather type contribute to the optimal use of water resources. With extensive crop cultivation, Khuzestan province is the central hub of agriculture, cereal production, and ultimately, its distributor to other provincial regions and Iran. The accurate ET estimation using RS can result in irrigation management, wheat water requirement supply, and optimal water use in a short temporal interval with a minimum economic cost. The climate of Khuzestan province is dry and hyperarid with annual evapotranspiration above 3000 mm and annual rainfall of 200 mm. Also, wheat is one of the most important strategic and widely consumed products (with extensive crop cultivation about 700–800 thousand hectares) in Iran, especially in Khuzestan province. Therefore, the evaluation of wheat evapotranspiration is necessary based on remote sensing algorithms and comparison with actual and empirical methods. Also, the evaluated results of the present algorithms in different researches are not the same and in many studies, the SEBAL algorithm has better results among the energy balance algorithms and in a number of others, the SEBS algorithm. In addition, in this research, remote sensing algorithms are investigated in comparison with various empirical methods categorized in the form of temperature, radiation, and mass transfer methods. Thus, it is essential to estimate the wheat crop ET based on SEBS and SEBAL algorithms compared to actual and empirical methods. Also, this topic has not been evaluated on the wheat crop in the study region, so far. Therefore, this work intends to:

- Estimating the wheat crop ET using SEBS and SEBAL algorithms.
- Comparing the ET estimated using SEBS and SEBAL algorithms with the lysimeter method.

- Comparing the SEBS and SEBAL-estimated ET with FAO-PM, Hargreaves-Samani, Blaney-Cridle, Doorenbos–Pruitt, Priestley-Taylor, Mahringer, and WMO empirical methods.

Materials and methods

Study area

Khuzestan province is located at 47° 41' to 50° 39' E from the prime meridian and 29° 58' to 33° 4' N from the equator in the southwest of Iran, with an area of about 64,057 km². The province shares borders with the Persian Gulf and Iraq in the south and west, respectively. In this study, daily weather data (2019–2020) were collected for the Shahid Modarres Basin in Ahvaz (Khuzestan province). The study area and the specifications of the studied station are represented in Fig. 1 and Table 1, respectively. The soil physico-chemical and irrigation water properties are also listed in Tables 2 and 3, respectively.

Data calculation

In this research, weather data were obtained from the Emam Khomeini agro industry Synoptic Station to implement the SEBS and SEBAL algorithms and evaluate the obtained results in comparison with other methods. Minimum and maximum air temperatures (°C), dew point temperature (°C), average relative humidity (%), maximum and minimum relative humidity (%), wind speed at the height of 2 m (m/s), number and maximum hours of sunshine, precipitation, and air pressure (Pa) were the data used in this study. These data were prepared from the mentioned synoptic station in Khuzestan province according to satellite passing days. The results of SEBS and SEBAL algorithms were compared by lysimeter and conventional empirical methods for ET estimation, including two temperature-based, two radiation-based, two mass transfer-based, and FAO-PM methods. Due to little incomplete (missing) data, they were estimated using appropriate renewal techniques (regression relative to the situation of each adjacent stations) and were controlled qualitatively before use. The ET obtained from SEBS and SEBAL algorithms were compared with all the mentioned methods using statistical indices to introduce the best method. To this aim, six Landsat 8 OLI satellite images (2019–2020) obtained from the US Geological Survey were used during the wheat growth period. It was attempted to select images with good cloudless weather conditions to provide ET comparisons. The accurate dates of the images used in this study are presented in Table 4.

To estimate actual ET, cloudless Landsat 8 satellite images were used during the wheat growth period

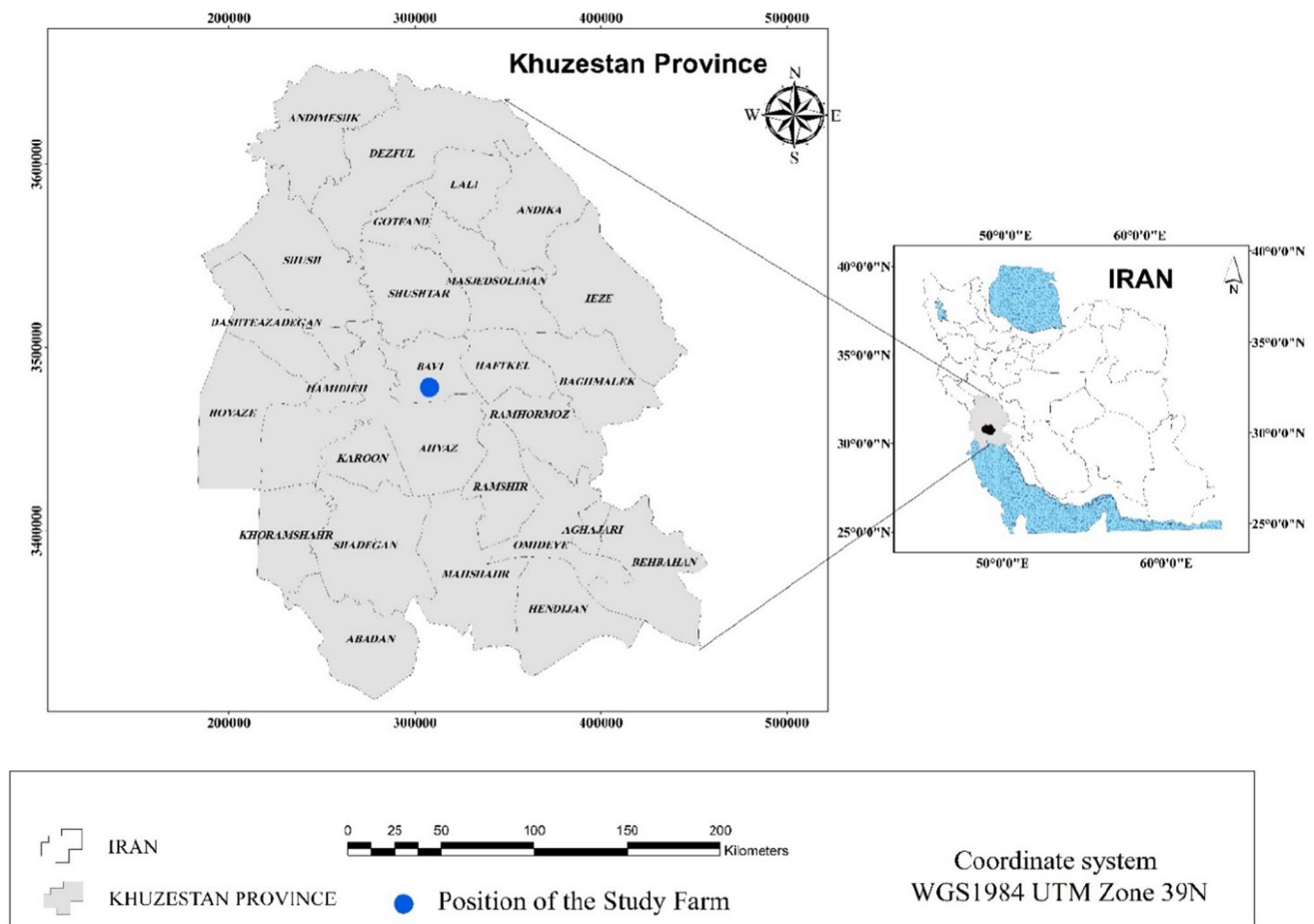


Fig. 1 The location of the study area in Khuzestan province of Iran

Table 1 Specifications of the study area located in Khuzestan province

Station	Longitude	Latitude	Elevation(mm)	Average annual precipitation (mm)	Dumarten coefficient	Period
Shahid Modarres Basin of Ahvaz	31° 20'	48° 40'	22.5	246.9	5.6	2019–2020

Table 2 Soil physical and chemical properties

Chemical properties	Physical properties
7.6 pH	1.65 Bulk density (g/cm^3)
4.8 (dS/m)Salinity	16 Clay(%)
0.4 Organic matter(%)	24 Silt(%)
	60 Sand(%)
	Sandy loam Soil texture

Table 3 Chemical properties of irrigation water

7.7	pH
4.8	EC (ds/m)
2.07	TDS (mg/l)
0.43	SAR
22	Ca (meq/l)
28	Mg (meq/l)
2.15	Na (meq/l)

Table 4 Meteorological statistics and the accurate dates of the images landsat 8

Date	Tmax(°C)	Tmin(°C)	RH(%)	U ₂ (m/s)	Hours of sunshine(hr)	P(kpa)
2019/11/27	17.1	11.4	80	5	0.0	100.9
2019/12/29	21.8	9.0	69	2	8.1	101.6
2020/01/30	22.2	7.4	68	2	8.4	101.7
2020/03/01	21.8	10.1	56	4	9.8	101.5
2020/04/03	29.9	17.6	37	4	11.1	101.1
2020/05/21	33.0	18.8	44	3	7.7	100.7

Table 5 Landsat 8 satellite characteristics

Date	Satellite	Spatial and temporal resolution	Percentage of cloud cover	Pass	Row
2019–11-27	Landsat8(OLI/TIRS)	30 m, 16 day	2.03	165	38
2019–12-29			2.16		
2020–01-30			5.96		
2020–03-01			13.32		
2020–04-03			1.22		
2020–05-21			0.22		

(November. 27 to May. 5 from 2019 to 2020). Since there are numerous errors in Landsat 8 images, the errors were eliminated by using two types of atmospheric and radiometric correction. The characteristics of the used images are shown in Table 5.

Surface Energy Balance Algorithm for Land (SEBAL)

The SEBAL algorithm provides a total balance of surface radiation and energy together with sensible heat flow and aerodynamic roughness, and ET is calculated as a component of energy per pixel. As mentioned, SEBAL includes an algorithm that solves complete energy balance (Eq. 1).

$$\lambda ET = R_n - G - H \tag{1}$$

where λET is the latent heat flux (W / m^2), R_n is the net radiations, G is the soil heat flux (W / m^2), and H is the sensible heat flux (W / m^2) (Bastiaanssen and Ali 2002).

Net solar radiation (Rn)

The R_n in each pixel was calculated using Eq. (2), where α is the surface albedo (dimensionless), $RS\downarrow$ is the incoming short wavelength radiation flux, $RL\downarrow$ is incoming wavelength radiation flux, $RL\uparrow$ is the outgoing long wavelength radiation flux, and ϵ_0 is the surface emissivity (a dimensionless quantity).

$$R_n = (1 - \alpha) RS\downarrow + RL\downarrow - RL\uparrow - (1 - \epsilon_0) RL\downarrow \tag{2}$$

In the following, the relationships required are introduced for the calculation of the five factors mentioned above.

Soil heat flux (SHF)

Directly, it is not possible to measure soil heat flux (SHF) using RS, but associations between the $\frac{G}{R_n}$ value and such factors as NDVI, surface temperature, and albedo have been reported in many investigations. In the present investigation, SHF was estimated with empirical Eq. (3) developed by Bastiaanssen 2000,

$$\frac{G}{R_n} = \frac{T_s}{\alpha} 0.0038\alpha + 0.0074\alpha 2(1 - 0.98NDVI4) \tag{3}$$

The Normalized Difference Vegetation Index (NDVI) is showed rate of vegetation coverage and its condition. This index estimates the earth's surface reflectance, leaf area index, area under cultivation, and plant biomass growth intensity (Bastiaanssen and Chandrapala 2003). The NDVI index is calculated by Eq. (4),

$$NDVI = \frac{NIR - R}{NIR + R} \tag{4}$$

where NIR and R are, respectively, reflectances in the near- and the red infrared bands. This index ranges between - 1 and + 1. Densely vegetated lands have positive values of 0.3 to 0.8, whereas negative values belong to snow-covered regions.

Sensible heat flux

The sensible heat flux of air value is obtained from wind speed and the earth surface temperature using a unique internal calibration consisting of the difference between the earth surface temperature and the adjacent air temperature (dT). The formula developed by Bastiaanssen 2000 is calculated through Eq. (5),

$$H = \frac{\rho_{air} \times C_p \times dT}{r_{ah}} \tag{5}$$

where ρ_{air} is air density (kg/m³), C_p indicates specific heat of the air (J/kg/K), dT represents temperature difference T_1 and T_2 (K) between two heights Z_1 and Z_2 , and r_{ah} is aerodynamic resistance to heat transport (sm⁻¹).

Surface Energy Balance System (SEBS)

The Surface Energy Balance System (SEBS) was proposed by Su and Jacobs 2001, to estimate heat flow fluxes and evaporative fractions. Similar to the SEBAL algorithm, the SEBS algorithm is based on the energy balance equation (Eq. 1). Among the components of the energy balance equation, the calculation method for net solar radiation (R_n) in SEBAL is identical to that of SEBS. To avoid repetition, the equations mentioned above are not presented in this section. Here, the equations are present for calculating two other components of the energy balance equation in the SEBS algorithm.

Soil heat flux (SHF)

Soil heat flux (SHF) in the SEBS algorithm is determined from Eq. (6),

$$G_0 = R_n [\Gamma_c + (1 - f_c) (\Gamma_s - \Gamma_c)] \tag{6}$$

where Γ_c is the ratio of SHF to net radiation (R_n) for dense vegetation, which is considered equal to 0.05. Γ_s is the ratio of SHF to R_n for bare soil, which is taken equal to 0.315, and f_c is the partial canopy coverage.

Sensible heat flux

In the SEBS algorithm, the sensible and latent heat flux are obtained from a similar theory. The definitions of planet

boundary layer (PBL), atmospheric boundary layer (ABL), and atmospheric surface layer (ASL) are differentiated in this algorithm. ABL refers to the part of the atmosphere directly affected by the earth's surface reactions and forces at a timescale below one hour. ASL represents the 10% lower ABL in which tensions and turbulent fluxes change less than 10%. In the ASL layer, the simulation relationships for the average wind speed profile (u) are written as Eq. 7.

$$u = \frac{u_*}{k} \left[\ln \left(\frac{z - d_0}{z_{om}} \right) - \Psi_m \left(\frac{z - d_0}{L} \right) + \Psi_m \left(\frac{z_{om}}{L} \right) \right] \tag{7}$$

In these equations, u and u_* represent wind speed and friction velocity (m/s), respectively, k is the von Karman constant equal to 0.4, z indicates the reference height (m), d_0 is the zero displacement height (m), z_{om} denotes roughness height for momentum (m), Ψ_m is the stability correction factor for atmospheric heat transfer, and L indicates the Monin–Obukhov length (m) (Su and Jacobs 2001).

To avoid the repeated introduction of more details on the applied equations, readers are referred to articles Bastiaanssen 2000; Bastiaanssen and Ali 2002 (for the SEBAL algorithm) and article Su and Jacobs 2001, (for the SEBS algorithm).

lysimeter

Cylindrical lysimeters (with 0.5 m diameter and 1.2 m height) were established to directly measure ET and crop coefficients. After grass and wheat crop ET (ET_c) measurements, crop coefficients (K_c) were obtained at each growth stage using Eq. (8),

$$K_c = \frac{ET_c}{ET_0} \tag{8}$$

where ET_c and ET_0 represent the evapotranspiration of the crop and reference crop (mm/day), respectively, and K_c is the crop coefficient (dimensionless).

Empirical methods of ET_0 estimation

In this research, the results of SEBS and SEBAL RS algorithms were evaluated using lysimeter and conventional empirical methods for ET_0 estimation to introduce the best method using statistical indices. The empirical methods used by each group are introduced in Tables 6, 7, 8.

Table 6 ET_0 estimation methods based on temperature

Dependent parameters	Reference	Formula	Method
T, u, Tmin, Tmax, RH, n, ϕ	Hargreaves–Samani(1985)	$ET_0 = 0.408 * 0.0025 * (T_a + 16.8) * (T_{max} - T_{min})^{0.5} * R_a$	Hargreaves–Samani
T, n, RHmin, ϕ , u	Blaney–Criddle(1950)	$ET_0 = a + b[P(0.46 T_a + 8.13)]$	Blaney–Criddle

Table 7 ET₀ estimation methods based on solar radiation

Dependent parameters	Reference	Formula	Method
RH, T, P, h, u, R _{nl} , R _{ns}	Priestley–Taylor(1972)	$ET_0 = \frac{\alpha}{\lambda} \frac{\Delta}{\Delta + \gamma} (R_n - G)$	Priestley–Taylor
RH, U, T, P, h, u, T _{min} , T _{max} , n, φ	Doorenbos–Pruitt(1977)	$ET_0 = a \left(\frac{\Delta}{\Delta + \gamma} R_s \right) + b$	Doorenbos–Pruitt

Table 8 ET₀ estimation methods based on mass transfer

Method	Formula	Reference	Dependent parameters
Mahringer	$ET_0 = 0.15072 \sqrt{3.6u} (e_s - e_a)$	Mahringer(1970)	T, T _{min} , T _{max} , RH, u
World meteorology organization (WMO)	$ET_0 = (0.1298 + 0.0934u) (e_s - e_a)$	World meteorology organization(1966)	T, T _{min} , T _{max} , RH, u

In Tables 6, 7, and 8, ET₀ is reference crop evapotranspiration (mm/day), T_a, T_{max}, T_{min}, and T_d are average, maximum, minimum, and dew point temperature, respectively (°C), R_a, extraterrestrial solar radiation (MJ/m²/day), a and b, empirical coefficients were presented by Doorenbos–Pruitt (1977), P, coefficient related to the length of the day, u, wind speed at the height of 2 m (m/s), n, actual sunshine duration (hr), φ, latitude (rad). RH, average relative humidity (%), R_s, solar radiation (MJ/m²/day), h, elevation of sea level (m), K and α, empirical coefficients, R_n, is net solar radiation (MJ/m²/day), e_{Smax} and e_{Smin}, maximum and minimum saturation vapor pressure, respectively (kPa), Δ represents the slope of the vapor pressure curve (kPa/°C), λ, latent heat of vaporization (MJ/kg), P, vapor pressure (kPa), R_{nl} and R_{ns}, net solar radiation with long and short wavelength, respectively (MJ/m²/day), e_s, and e_a, saturated and actual vapor pressure, respectively (kPa).

FAO-Penman–Monteith (FAO-PM) method

$$ET_0 = \frac{0.408\Delta(R_n - G) + \gamma \frac{900}{T+273} \times u_2(e_x - e_a)}{\Delta + \gamma(1 + 0.34u_2)} \tag{9}$$

In this method, Δ represents the slope of the vapor pressure curve (kPa/°C), R_n, is net solar radiation (MJ/m²/day), G is soil heat flux (MJ/m²/day), γ, psychrometric constants (kPa/°C), T, average air temperature (°C), u₂, average wind speed at a height of 2 m (m/s), e_s, saturated vapor pressure (kPa), e_a, actual vapor pressure (kPa), e_s - e_a, water vapor pressure deficiency(kPa).

If wind speed is measured at an height other than 2 m, it should be converted to speed at a 2 m height for use in the FAO-PM formula, the general equation of which is shown in the following:

$$U_{2m} = U_z \left[\frac{2}{Z} \right]^{0.2} \tag{10}$$

In this equation, U_{2m} and U_Z are, respectively, wind speeds at height of 2 and Z m, and Z is the height measured at which wind speed.

Since this study used data from weather stations, where wind speed is measured at 10 m height, the wind speed was converted to a 2 m height using Eq. (10).

Statistical indicators

To validate the results, the ET values estimated by SEBAL and SEBS algorithms were compared with lysimeter, FAO-PM, and empirical methods through conventional statistical indicators. In this investigation, the best method for the study area was determined using R², RMSE (mm/day), PBIAS (Lang et al. 2017), MBE, MAPE, and NS statistical indices (Ghaderi et al. 2020).

$$R^2 = \frac{[\sum_{i=1}^n (P_i - \bar{P})(O_i - \bar{O})]^2}{\sum_{i=1}^n (P_i - \bar{P})^2 \sum_{i=1}^n (O_i - \bar{O})^2} \tag{11}$$

$$RMSE = \sqrt{\frac{\sum_{i=1}^n (P_i - O_i)^2}{n}} \tag{12}$$

$$PBIAS = \frac{\sum_{i=1}^n O_i - P_i}{\sum_{i=1}^n O_i} \times 100 \tag{13}$$

$$MBE = \frac{1}{N} \sum_{i=1}^n O_i - P_i \tag{14}$$

$$MAPE = \left[\frac{1}{N} \sum_{i=1}^n \left| \frac{O_i - P_i}{O_i} \right| \right] \times 100 \tag{15}$$

Table 9 Wheat crop coefficients in different stages of growth

Date	Growth period (days)	K_c	Growth stage
2019/11/27	32	0.82	Initial
2019/12/29	42	1.35	Development
2020/01/30	42	1.20	Development
2020/03/01	42	1.06	Development
2020/04/03	48	1.03	Mid
2020/05/21	22	0.58	End

Table 10 Specifications of the limit values ET_c from satellite images

Date	Min		Max	
	SEBAL	SEBS	SEBAL	SEBS
2019–11-27	1.22	0.93	3.52	4.55
2019–12-29	0.28	1.10	2.83	3.95
2020–01-30	0.76	1.00	2.24	4.51
2020–03-01	0.96	1.40	4.62	5.80
2020–04-03	1.25	1.08	5.00	7.95
2020–05-21	1.29	1.00	3.72	3.74

$$NS = 1 - \left[\frac{\sum_{i=1}^n (O_i - P_i)^2}{\sum_{i=1}^n (O_i - \bar{O})^2} \right] \tag{16}$$

P_i and O_i are the values predicted with each RS algorithm and those obtained from comparative methods, respectively, \bar{P} and \bar{O} are the mean values predicted with each RS algorithm and those obtained from comparative methods, respectively, and n represents the total data.

Results and discussion

Crop coefficient

The wheat crop coefficient was calculated at each cultivation stage by considering reference crop ET as ET_0 and wheat crop ET of lysimeter data (ET_c). According to Table 9, the highest crop coefficient (k_c) belongs to the development stage on 29/12/2019 (42 days after cultivation), and the lowest level (0.58) was recorded for the final wheat growth period on 21/05/2020 (22 days after cultivation). The total actual ET was measured 460.1 mm during wheat cultivation for 144 days. The maximum and minimum water requirements were reported to be 231.23 and 19.47 mm/day during plant growth, respectively, in the Einkhosh Plain of Ilam in Iran (Ghaderi et al. 2020).

Also, the ET value of 203 mm was obtained for rainfed wheat for 155 days from November to April, in Khuzestan province (Porgholam Amiji et al., 2019). This difference can be attributed to cultivation conditions and time.

Calculation of wheat evapotranspiration using satellite image SV

To better illustrate different ET values during the growth period, the maximum and minimum values of wheat ET values are presented in Table 10. Accordingly, the minimum wheat ET values based on SEBAL and SEBS algorithms (0.28 and 0.93 mm/day) were recorded on December 29 and November 27, respectively. Moreover, the maximum wheat ET values based on SEBAL and SEBS algorithms (5 and 7.95 mm/day, respectively) occurred on April 03, 2020.

Figures 2 and 3 depict the spatiotemporal changes of daily ET values in the whole study area for SEBAL and SEBS algorithms, respectively. As shown in the figures, the ET dispersion obtained from SEBAL images is slightly more from SEBS images. Reasons of this observation may be a high estimation of the net radiation flux, which is confirmed by Wang et al. 2017 and Khand et al. 2021.

Comparison of evapotranspiration estimated with lysimeter method

Tables 11 and 12 compare the ET values estimated by SEBAL and SEBS algorithms with those of the lysimeter method. According to Table 11, the maximum ET values estimated by SEBAL and SEBS algorithms (16.67 and 14.21 mm/day, respectively), similar to the lysimeter (11.50 mm/day), were recorded on 2020/05/21. The minimum ET values estimated by these two algorithms (1.29 and 1.22 mm/day, respectively), similar to the lysimeter (1.70 mm/day), were documented on 2019/12/29.

Figure 4 displays the dispersion of ET values estimated by SEBAL and SEBS algorithms compared to the lysimeter method. As indicated by the assessments, SEBAL and SEBS algorithms correspond to the actual lysimeter method, and the results of energy balance algorithms can be generalized to the lysimeter method. These findings agree with those reported by Rawat et al. 2017, Asadi and Valizadeh Kamran. 2022, Tariqul Islam et al. 2023, Liu et al. 2023, and Khoshnood et al. 2023.

Table 12 compares R^2 and RMSE values obtained for SEBAL (0.92 and 2.15 mm/day) and SEBS (0.96 and 1.53 mm/day) algorithms with the lysimeter method. Thus, the estimated and observed ET values are close to each other on the mentioned days. Hence, SEBS and SEBAL algorithms are relatively good alternatives to the lysimeter

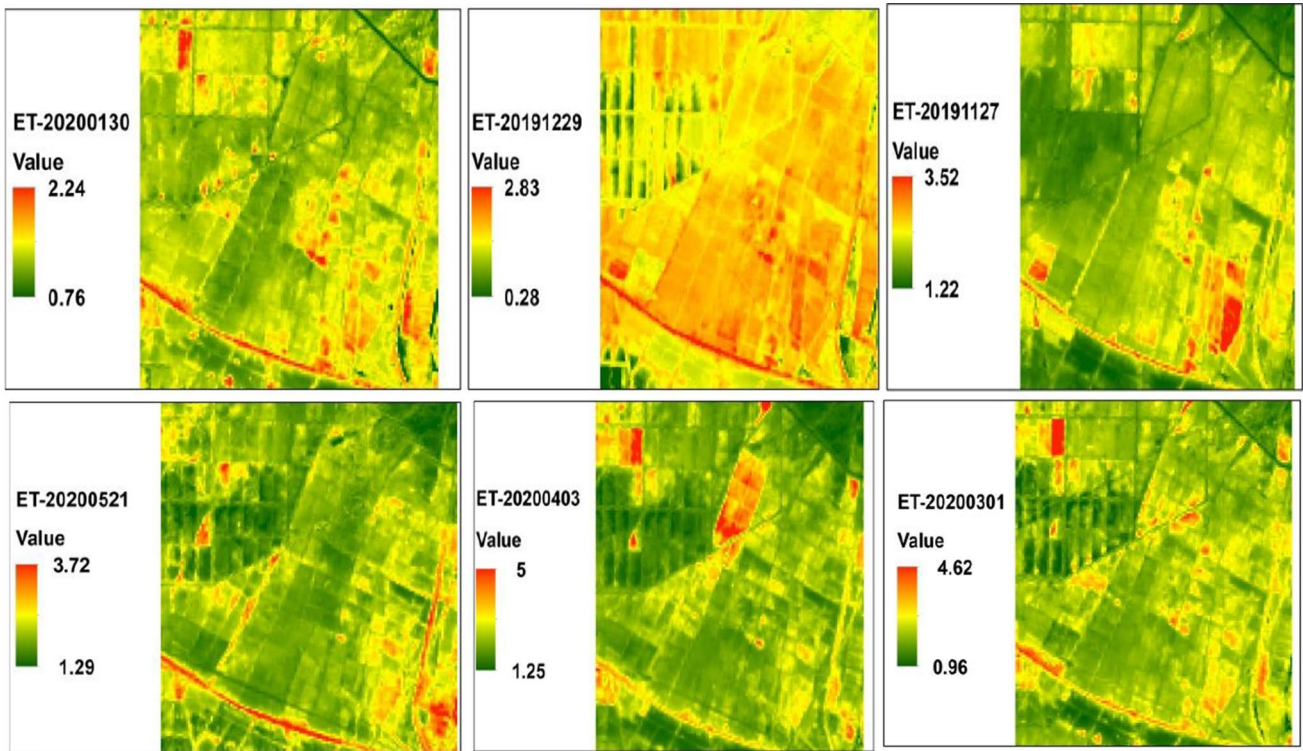


Fig. 2 The process of spatial and temporal changes of actual wheat ET using the SEBAL algorithm

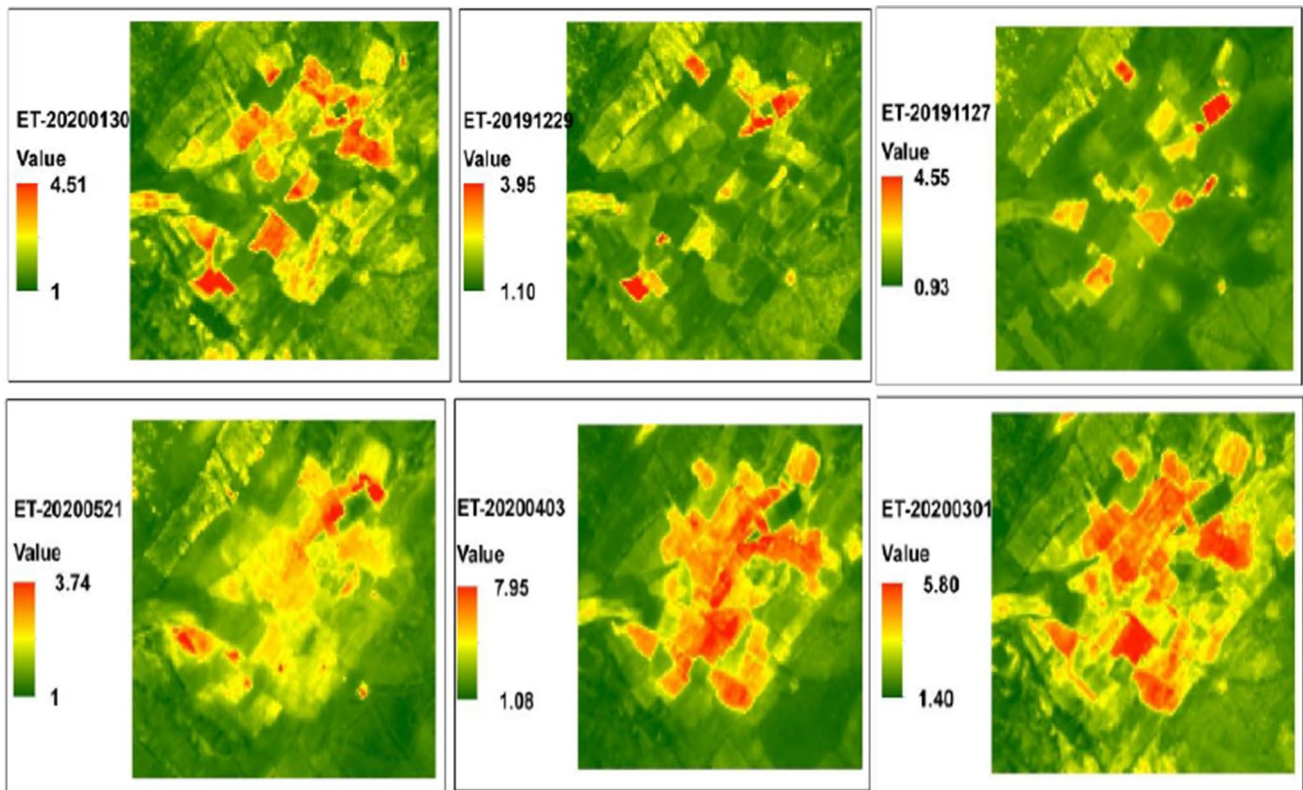


Fig. 3 The process of spatial and temporal changes of actual wheat ET using the SEBS algorithm

Table 11 Estimated actual ET values and lysimeter (mm/day)

Date	SEBAL	SEBS	Lysimeter
2019-11-27	2.27	2.33	2.07
2019-12-29	1.22	1.29	1.70
2020-01-30	3.03	3.86	3.50
2020-03-01	2.09	4.02	3.40
2020-04-03	4.08	5.73	6.21
2020-05-21	14.21	16.67	11.50

method and can be considered a valuable criterion compared to other empirical methods. Compared SEBAL (MBE = 0.25, MAPE = 25% and NS = 0.88) and SEBS (MBE = -0.92, MAPE = 20% and NS = 0.82), the lysimeter method showed good compatibility with the data of these two algorithms.

Comparison of evapotranspiration estimated and empirical methods

According to Table 13, the maximum ET values estimated from SEBS and SEBAL algorithms (16.67 and 14.21 mm/day, respectively) and empirical methods (except for the Blaney-Criddle method) were recorded on 2020/05/21. The minimum ET values estimated from SEBS and SEBAL algorithms (1.67 and 1.22 mm/day, respectively) were similar to FAO-PM (1.80 mm/day) on 2019/12/29. Figures 5 and 6 illustrate the dispersion of ET values estimated by SEBAL and SEBS algorithms compared to empirical methods. According to the evaluations, SEBAL and SEBS algorithms ($R^2 = 0.79$ and 0.87 , respectively) showed high compatibility with the FAO-PM method.

Among temperature-based methods, the Hargreaves-Samani method showed good accuracy compared to SEBAL ($R^2 = 0.72$) and SEBS ($R^2 = 0.80$) data.

Table 12 Comparison of estimated and lysimeter ET values using statistical indicators

Statistical indicators	Method											
	SEBAL						SEBS					
	R ²	RMSE	BIAS%	MBE	MAPE%	NS	R ²	RMSE	BIAS%	MBE	MAPE%	NS
Lysimeter	0.92	2.15	5.25	0.25	25	0.88	0.96	1.53	4.40	-0.92	20	0.82

Fig. 4 Scatter plot of ET estimated with SEBAL and SEBS algorithms and lysimeter method

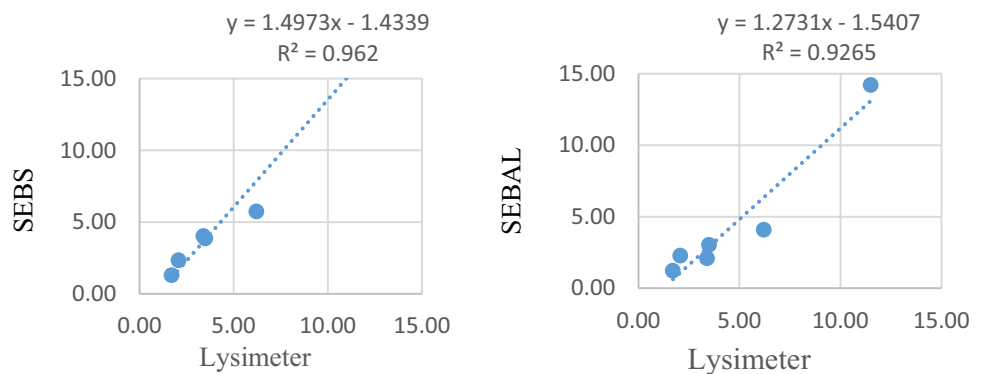


Table 13 Estimated and empirical values of actual ET (mm/day)

Date	SEBAL	SEBS	FAO-PM	Blaney—Criddle	Hargreaves-Samani	Priestley Taylor	Doorenbos and Pruitt	WMO	Mahringer
2019-11-27	2.27	2.33	1.95	2.12	1.45	1.14	1.31	0.36	0.39
2019-12-29	1.22	1.29	1.80	2.98	2.25	1.34	2.19	0.46	0.59
2020-01-30	3.03	3.86	2.65	3.85	2.54	1.39	2.55	0.52	0.67
2020-03-01	2.09	4.02	4.20	4.28	3.55	2.90	4.16	0.69	0.79
2020-04-03	4.08	5.73	6.15	7.65	5.32	4.46	6.45	1.11	1.26
2020-05-21	14.21	16.67	9.08	6.35	7.03	4.93	8.75	1.17	1.42

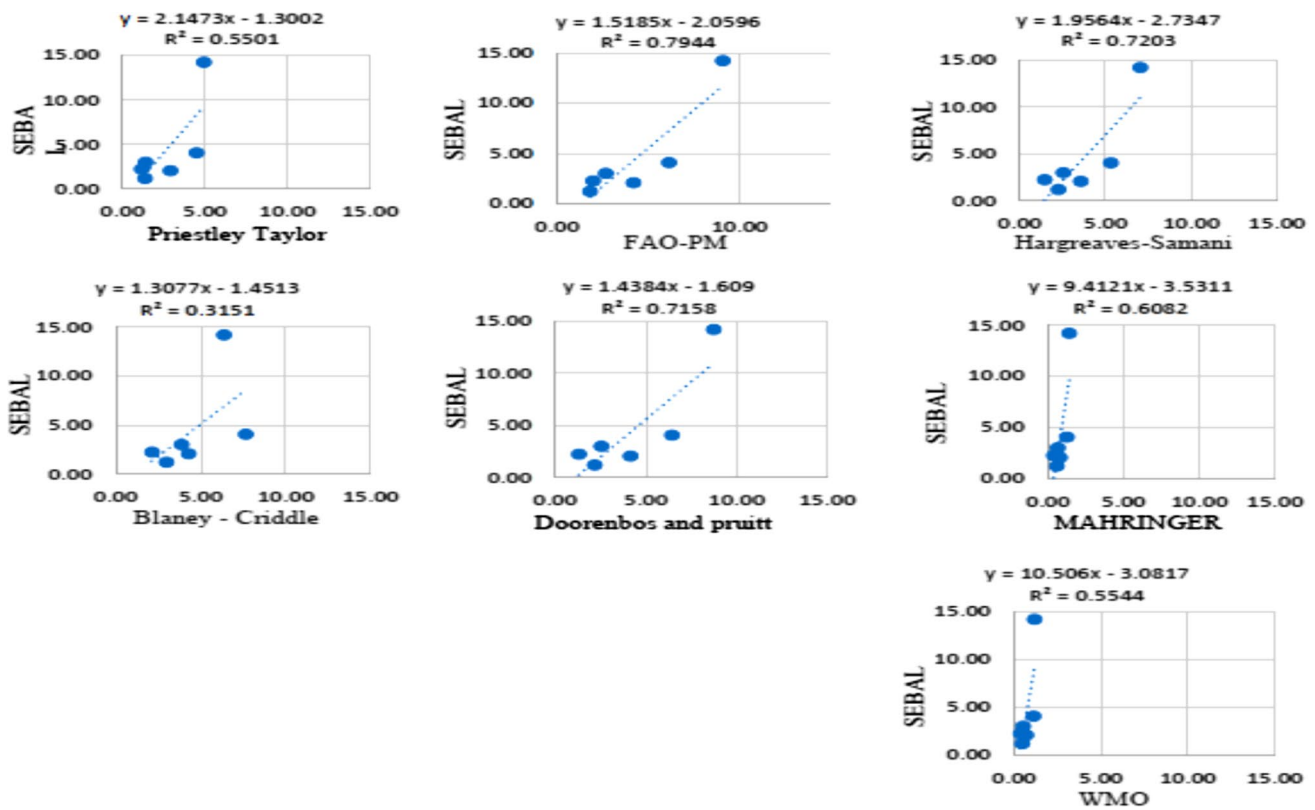


Fig. 5 Scatter plot of actual ET estimated with SEBAL algorithm and empirical methods

Also, in the temperature-based group, a weak estimation was observed for the Blaney-Criddle method relative to SEBAL and SEBS algorithms ($R^2=0.31$ and 0.39 , respectively). The reasons may include limited parameters in this method and its unsuitability according to the climate of the study area. Among radiation-based methods, the Doorenbos–Pruitt method showed good outcomes with SEBAL ($R^2=0.71$) and SEBS ($R^2=0.79$) data. Thus, the Doorenbos–Pruitt method performs better in arid climates among radiation-based methods and can be used for ET estimation in arid and semiarid areas. Additionally, the Doorenbos–Pruitt method needs more input parameters than the other methods, which can account for its improved efficiency compared to SEBS and SEBAL. In the mass transfer-based group, both Mahringer and WMO methods presented less effective estimations versus SEBAL ($R^2=0.60$ and 0.68 , respectively) and SEBS ($R^2=0.55$ and 0.64 , respectively). This might be due to the unsuitability of related parameters in mass transfer-based methods with energy balance algorithms in the study area. It is noteworthy that a limitation of SEBAL and SEBS algorithms is that the presence of some empirical relationships during ET estimation may result in errors. These models also require a bright cloudless sky because even a thin cloud layer can reduce the estimated heat radiation and

energy, leading to many errors. Therefore, better results were obtained with the Mahringer method among mass transfer-based methods. According to the results, SEBAL and SEBS algorithms mainly were compatible with the actual lysimeter method ($R^2=0.92$ and 0.96 , respectively). The high accuracy of these two algorithms in ET estimation suggests their copious applicability for studying large extents.

Table 14 compares the estimated data obtained from SEBAL and SEBS with ET data measured by the FAO-PM reference, Hargreaves-Samani, Blaney-Criddle, Priestley-Taylor, Doorenbos–Pruitt, Mahringer, and WMO methods.

According to Table 14, the RMSE values for the FAO-PM method were obtained at 2.42 and 3.14 mm/day for SEBS and SEBAL algorithms, respectively. The scatter plots (Figs. 5 and 6) represent less dispersion and more correlation of SEBS than SEBAL compared to the other methods. The scatter plots show higher R^2 and lower RMSE values for SEBS (with a slight difference) than SEBAL, with more acceptable accuracy closer to actual values. The PBIAS index also reveals underestimations for both SEBAL and SEBS, with a more significant underestimation for SEBAL. This result can be attributed to the high estimation of the net radiation flux parameter, the main factor among the fluxes in the energy balance equation, which has caused a more

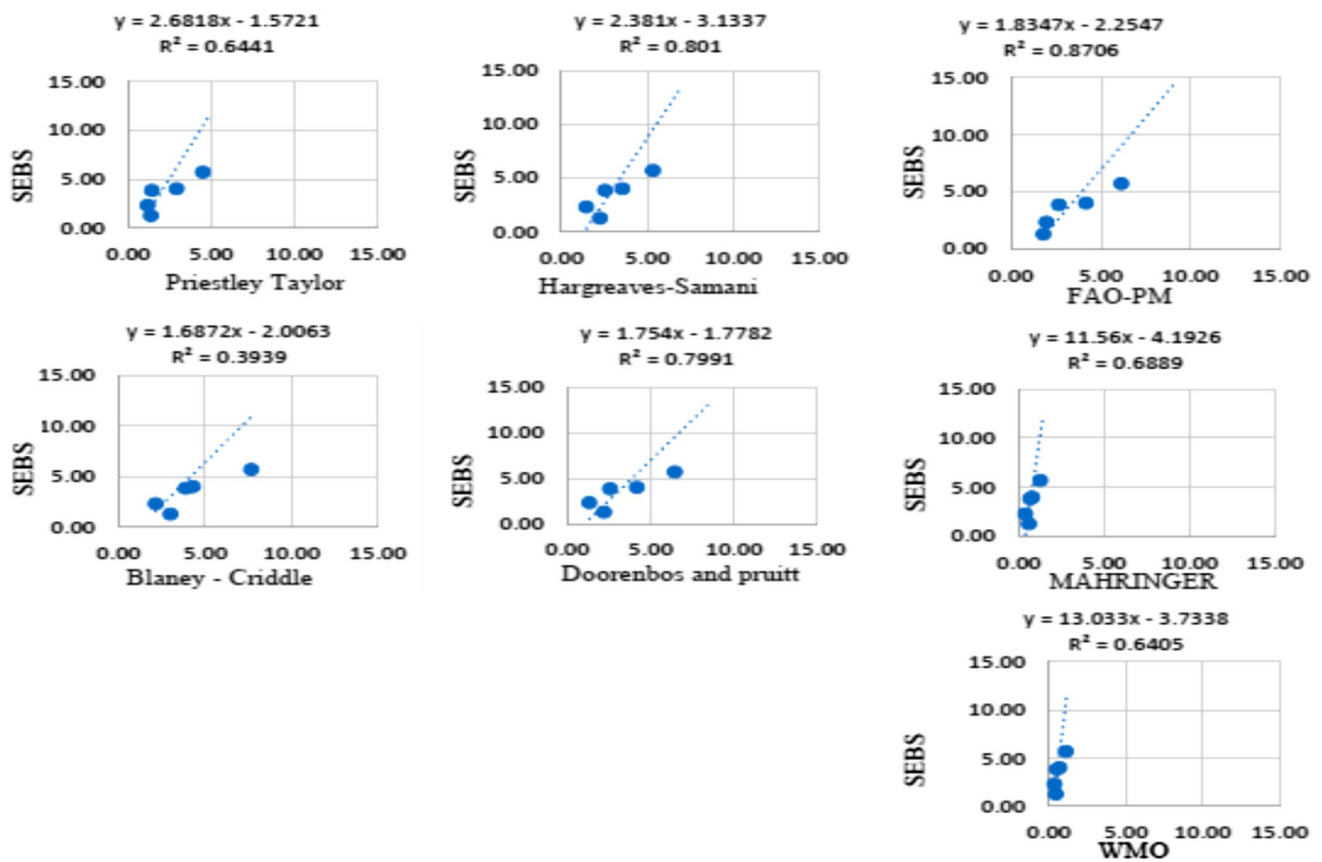


Fig. 6 Scatter plot of actual ET estimated with SEBS algorithm and empirical methods

Table 14 Comparison of estimated and empirical methods actual ET values using statistical indicators

Statistical indicators Methods	SEBAL						SEBS					
	R ²	RMSE	BIAS%	MBE	MAPE%	NS	R ²	RMSE	BIAS%	MBE	MAPE%	NS
(FAO-PM)	0.79	3.14	9.00	-1.17	33	0.70	0.87	2.42	7.47	-1.34	31	0.62
Hargreaves-Samani	0.72	16.4	16.77	1.79	48	0.52	0.80	10.4	18.50	-1.96	52	0.38
Blaney—Criddle	0.31	4.34	17.63	1.26	52	0.3	0.39	3.71	4.47	-1.11	43	0.28
Priestley Taylor	0.55	7.62	37.80	-2.25	75	0.23	0.64	3.89	29.20	-2.96	65	0.16
Doorenbos and Pruitt	0.71	3.33	21.36	-1.79	47	0.65	0.79	2.63	12.68	-1.43	46	0.58
Mahringer	0.60	6.80	35.36	-3.63	70	-0.55	0.68	5.51	32.36	-4.70	55	-0.76
WMO	0.55	6.93	32.53	-3.76	80	-0.62	0.64	5.64	29.35	-4.80	63	-0.83

significant underestimation of SEBAL than SEBS. It is noteworthy that the heat flux is low in farmlands or lands with intensive and semi-intensive vegetation. The soil heat flux is also low in densely vegetated lands. This is because the soil under vegetation is not exposed to radiation energy in dense vegetation, and the flux reaches a medium value with decreasing vegetation intensity. SHFs decline during the growing season because of plant growth and increasing crop coverage. The heat flux will be high in barren and arid zones. Thus, the SEBAL algorithm shows some underestimation

in comparison with direct and indirect methods, which can be attributed to a low SHF in the SEBAL model. Compared SEBAL (MBE = -1.17, MAPE = 33%, and NS = 0.70) and SEBS (MBE = -0.92, MAPE = 20%, and NS = 0.62) with empirical methods, the FAO-PM method showed the most compatibility with the data of these two algorithms among the other empirical methods. Based on the comparison of all tested methods with SEBAL (Table 15), the first, second, and third ranks belong to FAO-PM, Doorenbos–Pruitt, and Hargreaves-Samani methods, respectively, followed by

Table 15 Ranking the results of comparison empirical methods with the SEBAL algorithm

Statistical indicators	Methods							
	SEBAL							
	R^2	RMSE	BIAS%	MBE	MAPE%	NS	Ave	Rank
(FAO-PM)	1	1	1	1	1	1	1.0	1
Hargreaves-Samani	2	7	2	3	3	3	3.3	3
Blaney—Criddle	6	3	3	2	4	4	3.6	4
Priestley Taylor	5	6	7	4	5	5	5.3	6
Doorenbos and Pruitt	3	2	4	3	2	2	2.6	2
Mahringer	4	4	6	5	6	6	5.1	5
WMO	5	5	5	6	7	7	5.8	7

Table 16 Ranking the results of comparison empirical methods with the SEBS algorithm

Statistical indicators	Methods							
	SEBS							
	R^2	RMSE	BIAS%	MBE	MAPE%	NS	Ave	Rank
(FAO-PM)	1	1	2	2	1	1	1.3	1
Hargreaves-Samani	2	7	4	4	4	3	4	4
Blaney—Criddle	6	3	1	1	2	4	2.8	3
Priestley Taylor	5	4	5	5	7	5	5.1	5
Doorenbos and Pruitt	3	2	3	3	3	2	2.6	2
Mahringer	4	5	7	6	5	6	5.5	6
WMO	5	6	6	7	6	7	6.1	7

Blaney-Criddle, Mahringer, Priestley-Taylor, and WMO empirical methods in order. Moreover, the comparison of all tested empirical methods with SEBS in Table 16 indicates that FAO-PM, Doorenbos–Pruitt, and Blaney-Criddle are in the first, second, and third ranks, respectively, followed by Hargreaves-Samani, Priestley-Taylor, Mahringer, and WMO empirical methods in order. Tables 15 and 16 show the satisfactory results of the ET values estimated from SEBS and SEBAL compared to the FAO-PM empirical method. Since FAO-PM has been introduced as one of the most reliable reference methods in ET calculations, validation with this method is also important and helpful when direct land measurement data (lysimeter) are not available. During the wheat growth, the highest ET values with SEBS (16.67 mm/day) and SEBAL (14.21 mm/day) correspond to the maximum values with lysimeter (11.50 mm/day) and FAO-PM (9.08 mm/day) at the final growth phase on 2020/05/21 (Tables 11 and 13). These tables also indicate that the minimum wheat ET values with SEBS (1.29 mm/day) and SEBAL (1.22 mm/day) at the development phase match with the least values with lysimeter (1.70 mm/day) and FAO-PM (1.80 mm/day) on 2020/05/21. The results demonstrate the acceptable performance of energy balance algorithms in ETc estimation. The SEBS shows higher precision than SEBAL in ET estimation compared to the data of the lysimeter and FAO-PM, which yielded better results than the other empirical methods. Previous studies (Wang et al. 2017, Rawat et al.

2017, Khand et al. 2021, Yang et al. 2022, Wei et al. 2022, Liu et al. 2023, and Khoshnood et al. 2023) suggest the ability of energy balance algorithms, in particular SEBS, in crop actual ET estimation. Among temperature-based methods, the Hargreaves-Samani showed better performance, which agrees with Lang et al. 2017, and Zoratipour et al. 2019. Among radiation-based methods, the Doorenbos–Pruitt performed better than the Priestley-Taylor, which is similar to its good performance in ET estimation reported by Wang et al. 2017, Zoratipour et al. 2019, and Shamloo et al. 2021. Among mass transfer-based methods, the Mahringer method presented a better estimation, as reported by Djaman et al. 2015 and Zoratipour et al. 2019.

Conclusion

In this research, wheat daily ET values were estimated accurately using SEBAL and SEBS algorithms as well as Landsat 8 satellite images at six satellite passing dates from 2019 to 2020, and their results were compared with the lysimeter method. The results demonstrated that the ETc estimated with SEBS and SEBAL ($R^2=0.96$ and 0.92 , $RMSE=1.53$ and 2.42 mm/day, respectively) corresponded well to actual lysimeter data and can be compared with empirical methods. Therefore, SEBS and SEBAL results were compared with FAO-PM, Hargreaves-Samani, and Blaney-Criddle

temperature-based methods, Priestley-Taylor and Doorenbos–Pruitt radiation-based methods, and Mahringer and WMO mass transfer-based methods, using statistical indices. Based on the findings, FAO-PM showed good compatibility with SEBS and SEBAL ($R^2=0.87$ and 0.79 , $RMSE=2.42$ and 3.14 mm/day, respectively) among the mentioned empirical methods. Altogether, the ET values obtained from SEBAL, SEBS, and the lysimeter method (26.9, 33.9, and 28.38 mm/day, respectively) were not highly different. In addition, the ET value estimated from SEBS is about 12% higher than that obtained from SEBAL. Thus, SEBS with more outstanding scores ($R^2=0.96$ and $RMSE=1.53$ mm/day) presented better results than SEBAL. Compared to the lysimeter method, SEBS and SEBAL algorithms are appropriate alternatives for use in the study area owing to their high compatibility in the absence of adequate data and no use of direct methods.

Acknowledgements This paper is derived from a research project with the number 1349, for which the authors are grateful to the Research Council of Shahid Chamran University of Ahvaz for financial support (GN: SCU.WI1400.273).

Data availability The datasets generated and/or analyzed during the current study are available upon request by contact with the corresponding author.

Declarations

Conflict of interest The authors declare that they have no known competing financial interests or personal relationships that could have appeared to influence the work reported in this paper.

Ethical approval This manuscript does not involve ethical approval.

Consent to publish All authors have read and agreed to the published version of the manuscript.

Open Access This article is licensed under a Creative Commons Attribution 4.0 International License, which permits use, sharing, adaptation, distribution and reproduction in any medium or format, as long as you give appropriate credit to the original author(s) and the source, provide a link to the Creative Commons licence, and indicate if changes were made. The images or other third party material in this article are included in the article's Creative Commons licence, unless indicated otherwise in a credit line to the material. If material is not included in the article's Creative Commons licence and your intended use is not permitted by statutory regulation or exceeds the permitted use, you will need to obtain permission directly from the copyright holder. To view a copy of this licence, visit <http://creativecommons.org/licenses/by/4.0/>.

References

- Allen RG, Morse A, Tasumi M, Trezza R, Bastiaanssen W, Wright JL, Kramber W (2002) Evapotranspiration from a satellite-based surface energy balance for the Snake Plain Aquifer in Idaho. In: Proceeding USCID conference 167–178
- Asadi M, Valizadeh Kamran K (2022) Comparison of SEBAL, METRIC, and ALARM algorithms for estimating actual evapotranspiration of wheat crop. *Theor Appl Climatol*. <https://doi.org/10.1007/s00704-022-04026-3>
- Bastiaanssen WG (2000) SEBAL-based sensible and latent heat fluxes in the irrigated Gediz Basin. *Turkey J Hydrol* 229(1–2):87–100. [https://doi.org/10.1016/S0022-1694\(99\)00202-4](https://doi.org/10.1016/S0022-1694(99)00202-4)
- Bastiaanssen WGM, Ali S (2002) A new crop yield forecasting model based on satellite measurements applied across the Indus Basin, Pakistan. *Agr Ecosyst Environ* 94:321–343. [https://doi.org/10.1016/S0167-8809\(02\)00034-8](https://doi.org/10.1016/S0167-8809(02)00034-8)
- Bastiaanssen WGM, Chandrapala L (2003) Water balance variability across Sri Lanka for assessing agricultural and environmental water use. *Agr Water Manag* 58(2):171–291. [https://doi.org/10.1016/S0378-3774\(02\)00128-2](https://doi.org/10.1016/S0378-3774(02)00128-2)
- Blaney HF, Criddle WD (1950) Determining water requirements in irrigated areas from climatological and irrigation data. Soil conservation service technical paper 96; Soil conservation service. US Department of Agriculture, Washington
- Djaman KB, Alde AB, Sow A, Muller F, Irmak S, Ndiaye MK, Manneh B, Moukoubi YD, Futakuchi K, Saito K (2015) Evaluation of sixteen reference evapotranspiration methods under Sahelian conditions in the Senegal river valley. *J Hydrol Reg Stud* 78:139–159. <https://doi.org/10.1016/j.ejrh.2015.02.002>
- Doorenbos J, Pruitt WO (1977) Crop water requirements. FAO Irrigation and Drainage. Paper no. 24 (rev.). FAO, Rome.
- Elmer A, Khadr M, Kana S, Tawfik A (2019) Mapping daily and seasonally evapotranspiration using remote sensing techniques over the Nile delta. *Agr Water Manag* 213:682–692. <https://doi.org/10.1016/j.agwat.2018.11.009>
- Ghaderi A, Dasineh M, Shokri M, Abraham J (2020) Estimation of actual evapotranspiration using the remote sensing method and SEBAL algorithm: a case study in Ein Khosh Plain Iran. *Hydrology* 7(36):1–14. <https://doi.org/10.3390/hydrology7020036>
- Hargreaves GL, Samani ZA (1985) Reference crop evapotranspiration from temperature. *Appl Eng Agric* 1(2):96–99. <https://doi.org/10.13031/2013.26773>
- Khand K, Bhattarai N, Taghvaeian S, Wagle P, Gowda PH, Alderman PD (2021) Modeling evapotranspiration of winter wheat using contextual and pixel-based surface energy balance models. *Trans ASABE* 64(2):507–519
- Khoshnood S, Lotfata A, Mombeni M, Daneshi A, Verrelst J, Ghorbani K (2023) A spatial and temporal correlation between remotely sensing evapotranspiration with land use and land cover. *Water* 15(1068):1–20. <https://doi.org/10.3390/w15061068>
- Lang D, Zheng J, Shi J, Liao F, Ma X, Wang W, Chen X, Zhang M (2017) A comparative study of potential evapotranspiration estimation by eight methods with FAO Penman-Monteith method in South Western China. *Water J* 74:1–18. <https://doi.org/10.3390/w9100734>
- Lian J, Huang M (2015) Evapotranspiration estimation for an oasis area in the Heihe river basin using landsat 8 images and the METRIC model. *Water Resour Manag* 29(14):5157–5170. <https://doi.org/10.1007/s11269-015-1110-z>
- Liu R, Jiao L, Liu Y, Wang Y (2023) Multi-scale spatial analysis of satellite-retrieved surface evapotranspiration in Beijing, a rapidly urbanizing region under continental monsoon climate. *Environ Sci Pollut Res* 30:20402–20414. <https://doi.org/10.1007/s11356-022-23580-x>
- Mahringer W (1970) Verdunstungsstudien am neusiedler see. *Arch Met Geoph Biokl Ser b* 18:1–20. <https://doi.org/10.1007/BF02245865>
- Mattar MA, Alazba AA, Alblewi B, Gharabaghi B, Yassin MA (2016) Evaluating and calibrating reference evapotranspiration models using water balance under hyper-arid environment.

- Water Resour Manage 30:3745–3767. <https://doi.org/10.1007/s11269-016-1382-y>
- Obada E, Alamou EA, Chabi A, Zandagba J, Afouda A (2017) Trends and changes in recent and future Penman–Monteith potential evapotranspiration in Benin (West Africa). *J Hydrol* 4(38):1–18. <https://doi.org/10.3390/hydrology4030038>
- Pourgholam Amiji M, Hooshmand M, Raja O, Liaghat A (2019) Effective Rain Zoning in Khuzestan province under autumn rainfed wheat cultivation. *J Water and Irrig Manag* 2(9):211–230. <https://doi.org/10.22059/jwim.2019.290773.718>
- Priestley CHB, Taylor RJ (1972) On the assessment of surface heat flux and evapotranspiration using large scale parameters. *Mon Weather Rev* 100:81–92. [https://doi.org/10.1175/1520-0493\(1972\)100<3c0081:OTAOSH%3e2.3.CO;2](https://doi.org/10.1175/1520-0493(1972)100<3c0081:OTAOSH%3e2.3.CO;2)
- Racz C, Nagy J, Dobos AC (2013) Comparison of several methods for calculation of reference evapotranspiration. *Acta Silv Lign Hung* 9:9–24. <https://doi.org/10.2478/aslh-2013-0001>
- Rawat KS, Bala A, Singh SK, Pal RK (2017) Quantification of wheat crop evapotranspiration and mapping: a case study from Bhiwani District of Haryana, India. *Agr Water Manag* 187:200–209. <https://doi.org/10.1016/j.agwat.2017.03.015>
- Saboori M, Mokhtari A, Afrasiabian Y, Daccache A, Alaghmand S, Mousivand Y (2021) Automatically selecting hot and cold pixels for satellite actual evapotranspiration estimation under different topographic and climatic conditions. *Agr Water Manag* 248(106763):1–20. <https://doi.org/10.1016/j.agwat.2021.106763>
- Shamloo N, Taghi Sattari M, Apaydin H, Valizadeh Kamran K, Prasad R (2021) Evapotranspiration estimation using SEBAL algorithm integrated with remote sensing and experimental methods. *Int J Digit Earth* 14(11):1638–1658. <https://doi.org/10.1080/17538947.2021.1962996>
- Su Z, Jacobs C (2001) Advanced earth observation-land surface climate; final report (No. 01–02)
- Tan L, Zheng K, Zhao Q, Wu Y (2021) Evapotranspiration estimation using remote sensing technology based on a SEBAL model in the upper reaches of the Huaihe river basin. *Atmosphere* 12(1599):1–17. <https://doi.org/10.3390/atmos12121599>
- Tariqul Islam AFM, Saiful Islam AKM, Tarekul Islam GM, Kumar Bala S, Salhin M, Kanti Choudhury A, Dey N, Golam Mahboob M (2023) Simulation of water productivity of wheat in north-western Bangladesh using multi-satellite data. *Agr Water Manag* 281(108242):1–16. <https://doi.org/10.1016/j.agwat.2023.108242>
- Temesgen E (2009) Estimation of evapotranspiration from satellite remote sensing and meteorological data over the Fogera Floodplain-Ethiopia. Dissertation, International institute for geoinformation science and earth observation (ITC), Enschede, The Netherlands
- Valipour M (2017) Calibration of mass transfer-based models to predict reference crop evapotranspiration. *Appl Water Sci* 7:625–635. <https://doi.org/10.1007/s13201-015-0274-2>
- Wang Q, Blackburn GA, Onojeghuo AO, Dash J, Zhou L, Zhang Y, Atkinson PM (2017) Fusion of Landsat8 OLI and Sentinel2 MSI data. *IEEE Trans Geosci Remote Sens* 55(7):3885–3899. <https://doi.org/10.1109/TGRS.2017.2683444>
- Wei G, Cao J, Xie H, Xie H, Yang Y, Wu C, Cui Y, Luo Y (2022) Spatial-temporal variation in paddy evapotranspiration in subtropical climate regions based on the SEBAL model: a case study of the Ganfu plain irrigation system Southern China. *Remote Sens* 14(1201):1–19. <https://doi.org/10.3390/rs14051201>
- WMO (1966) Measurement and estimation of evaporation and evapotranspiration. Tech Pap. (CIMO-Rep) 83. Genf
- Wolff W, Francisco J, Flumignan D, Marin F, Folegatti M (2022) Optimized algorithm for evapotranspiration retrieval via remote sensing. *Agr Water Manag* 262(107390):1–13. <https://doi.org/10.1016/j.agwat.2021.107390>
- Xu CY, Singh VP (2002) Cross comparison of empirical equations for calculating potential evapotranspiration with data from Switzerland. *Water Resour Manag* 16:197–219. <https://doi.org/10.1023/A:1020282515975>
- Yang L, Li J, Sun Z, Liu J, Yang Y, Li T (2022) Daily actual evapotranspiration estimation of different land use types based on SEBAL model in the agro-pastoral ecotone of northwest China. *PLoS ONE*. <https://doi.org/10.1371/journal.pone.0265138>
- Zoratipour E, Soltani A, Zoratipour A (2019) Spatial and temporal evaluation of different methods for prediction of reference evapotranspiration (case study: Khuzestan province). *Iran J Ecohydrol* 6(2):465–478. <https://doi.org/10.22059/ije.2019.272676.1017>

Publisher's Note Springer Nature remains neutral with regard to jurisdictional claims in published maps and institutional affiliations.